Proteolytic Maturation of $\alpha_2\delta$ Controls the Probability of Synaptic Vesicular Release

Authors: Laurent Ferron [1], Ivan Kadurin and Annette C. Dolphin

Department of Neuroscience, Physiology and Pharmacology, University College London, London WC1E 6BT, UK.

[1] **Correspondence and Materials**: Laurent Ferron (l.ferron@ucl.ac.uk), Department of Neuroscience, Physiology and Pharmacology, University College London, Gower Street, London, WC1E 6BT, UK Tel: +44-20-7679 3620

Running Title: Proteolysis of $\alpha_2\delta$-1 subunit is key to vesicular release

Number of words: Abstract (148), Introduction (479), Results (753) and Discussion (1643)

References: 61

Number of pages: 22 including Figures

Number of figures: 4

Conflict of Interest None

Abstract

Auxiliary $\alpha_2\delta$ subunits are important proteins for trafficking of voltage-gated calcium channels (Ca_V) at the active zones of synapses. We have previously shown that the post-translational proteolytic cleavage of $\alpha_2\delta$ is essential for their modulatory effects on the trafficking of N-type ($Ca_V2.2$) calcium channels (Kadurin et al. 2016). We extend these results here by showing that the probability of presynaptic vesicular release is reduced when an uncleaved $\alpha_2\delta$ is expressed in rat neurons and that this inhibitory effect is reversed when cleavage of $\alpha_2\delta$ is restored. We also show that asynchronous release is influenced by the maturation of $\alpha_2\delta$-1, highlighting the role of Ca_V channels in this component of vesicular release. We present additional evidence that $Ca_V2.2$ co-immunoprecipitates preferentially with cleaved wild-type $\alpha_2\delta$. Our data indicate that the proteolytic maturation increases the association of $\alpha_2\delta$-1 with Ca_V channel complex and is essential for its function on synaptic release.

Key words: calcium channel, $\alpha_2\delta$ subunit, proteolytic processing, synaptic transmission, vesicular release.

Introduction

Among the three families of Ca_V channels (Ca_V1, Ca_V2 and Ca_V3), the Ca_V2 family and more specifically $Ca_V2.1$and $Ca_V2.2$ channels (generating P/Q and N-type currents, respectively) are particularly important for synaptic transmission in central and peripheral nervous systems (Dolphin 2012). $Ca_V2.1$ and $Ca_V2.2$ are targeted to presynaptic terminals where they are responsible for triggering vesicular release (Catterall & Few 2008, Zamponi et al. 2015). Ca_Vs are formed of several subunits: the α_1 subunit, that constitutes the Ca^{2+} selective pore and the voltage sensor, and auxiliary subunits β (cytoplasmic) and $\alpha_2\delta$ (extracellular) (Flockerzi et al. 1986, Liu et al. 1996, Takahashi & Catterall 1987, Witcher et al. 1993). Four genes coding for $\alpha_2\delta$ subunits have been identified (Dolphin 2012). They are translated into a single pre-protein $\alpha_2\delta$ and post-translationally cleaved into α_2 and δ peptides which remain attached by di-sulfide bonds (Dolphin 2012). In $\alpha_2\delta$-1 and -2, α_2 contains a perfect metal ion adhesion site (MIDAS) motif essential for the interaction with α_1 subunit (Canti et al. 2005, Hendrich et al. 2008) and δ which is glycophosphatidylinositol (GPI) anchored to the plasma membrane (Davies et al. 2010). The structure of the $Ca_V1.1$ channel complex has been recently determined using cryo-electron microscopy and has identified binding domains between $Ca_V1.1$ and $\alpha_2\delta$-1 including the interaction of the $\alpha_2\delta$ MIDAS motif with loop I of the first repeated domain of Cav1.1 (Wu et al. 2016). Site-directed mutagenesis studies have confirmed a functional interaction between $\alpha_2\delta$-1 and the first extracellular loop of $Ca_V1.2$ (Bourdin et al. 2017) and $Ca_V2.2$ channels (unpublished results). $\alpha_2\delta$ subunits are important for the trafficking of α_1 subunits and their function, and they are also key proteins for synaptic function and synaptogenesis (Dickman et al. 2008, Eroglu et al. 2009, Hoppa et al. 2012, Saheki & Bargmann 2009, Zamponi et al. 2015). We have recently shown that the proteolytic maturation of $\alpha_2\delta$-1 into disulfide-linked polypeptides α_2 and δ is an essential post-translational step enabling its modulatory effect on the activation

and trafficking of N-type calcium channels in neurons (Kadurin et al. 2016). Indeed, we show that uncleaved $\alpha_2\delta$-1 inhibits presynaptic calcium transient triggered AP in hippocampal neurons and that this effect is reversed by the cleavage of $\alpha_2\delta$-1.

Here we investigate the impact of the proteolytic maturation of $\alpha_2\delta$-1 on synaptic release. We used optical tools to measure vesicular release parameters (Ariel & Ryan 2010, Hoppa et al. 2012). Our data show that an uncleaved $\alpha_2\delta$-1 reduces the probability of release in response to a single action potential, and also affects asynchronous release. These effects on presynaptic vesicular release are reversed when the cleavage of $\alpha_2\delta$-1 is restored. We provide additional evidence that cleaved $\alpha_2\delta$-1 interacts more than the uncleaved form with the $Ca_V2.2$ channel pore-forming subunit. Our data indicate that the proteolytic maturation of $\alpha_2\delta$-1 is important for its association with Ca_V channel complex and its function on synaptic release.

Results

$\alpha_2\delta$ subunits play a crucial role in the trafficking of fully functional calcium channels to the plasma membrane and to presynaptic terminals (Dolphin 2012). In order to determine the physiological impact of proteolytic maturation of $\alpha_2\delta$-1, we used the cleavage site mutant α_2(3C)δ-1 (Kadurin et al. 2016), which is resistant to endogenous proteolysis between α_2 and δ, to assess the effect of controlled cleavage by exogenous 3C-protease on vesicular release from presynaptic terminals, using the optical reporter vGlut-pHluorin. Transfected hippocampal neurons were identified by mCherry expression (Figure 1a). Neurons were subsequently stimulated (100 action potentials, AP, at 10 Hz), and fluorescence of vGlut-pHluorin was monitored to identify functional boutons (Figure 1a). We first examined the effect of expression of α_2(3C)δ-1 on synaptic release properties by measuring single AP-evoked exocytosis (Figure 1b). Single AP stimulations were repeated 10 to 12 times with a

45 s rest between each trials. Signals from each bouton were averaged and normalized to the fluorescence value obtained by rapid alkalinization of the entire labeled vesicle pool using NH_4Cl (Figure 1a and 1b). Overexpression of uncleaved α_2(3C)δ-1 induced a decrease of 29 ± 6 % in exocytosis compared to the control empty vector condition (n = 28 and 41, respectively; *P* = 0.04) (Figure 1c). Conversely, inducing controlled cleavage of α_2(3C)δ-1 by co-expressing 3C-protease resulted in an increase of 53 ± 18 % in exocytosis compared to α_2(3C)δ-1 alone (n = 41 and 16, respectively; *P* = 0.014), thus completely reversing the inhibitory effect of uncleaved α_2(3C)δ-1 (Figure 1b and 1c).

Synaptic vesicle exocytosis properties are determined by the number of vesicles available for rapid release (the readily-releasable pool - RRP) and the probability (*Pv*) that a vesicle in the RRP will undergo fusion in response to a single AP stimulus (Schneggenburger et al. 2002). RRP can be determined using a high frequency stimulation (Ariel & Ryan 2010, Ariel et al. 2012). During a 20 AP stimulus at 100 Hz, the fluorescence of vGlut-pHluorin in presynaptic terminals rapidly increases and reaches a plateau phase corresponding to the RRP (Figure 2a). The averaged response, obtained from 5-6 trials with a 5 min rest between each trial, were normalized to the size of the total presynaptic pool obtained with NH_4Cl application (Figure 2a). To examine whether proteolytic maturation of $\alpha_2\delta$-1 affects the size of the RRP, we imaged neurons transfected with either empty vector (Figure 2a) or α_2(3C)δ-1 (Figure 2b) or α_2(3C)δ-1 together with 3C-protease (Figure 2c) and compared the size of the RRP. As summarized in Figure 2d, no difference was recorded between the 3 conditions (empty vector, α_2(3C)δ-1 and α_2(3C)δ-1 with 3C-protease: 6.9 ± 0.4 %, 6.2 ± 0.3 % and 6.4 ± 0.5 % of total pool, n = 22, 16 and 19, respectively, *P* = 0.78), indicating that proteolytic maturation of $\alpha_2\delta$-1 affects the *Pv*, rather than the size of the RRP.

After the plateau phase corresponding to the RRP, an additional increase in fluorescence takes place during the stimulation, and continues for more than 500 ms after the end of the stimulus before reaching a stationary phase (Figure 3a). It was proposed that this secondary

increase in fluorescence results from a combination of RRP refilling and slow decay of the elevated intracellular Ca^{2+} concentration (Ariel & Ryan 2010). This late increase in fluorescence occurs at lower rate than the initial increase and represents post-stimulus exocytosis. Overexpression of uncleaved α_2(3C)δ-1 induced a decrease of about 30 % in this phase of exocytosis compared to control empty vector condition (n = 22 and 31, respectively; $P < 0.001$) (Figure 3b-c). This reduction of delayed exocytosis is completely prevented by the co-expression of α_2(3C)δ-1 with 3C-protease (Figure 3a-b).

We then wished to determine whether the results obtained on presynaptic release were due to differential interaction of cleaved and uncleaved $\alpha_2\delta$ with the α1 subunit. We have previously shown that transient expression of $\alpha_2\delta$-1 in cell lines results in only a partial cleavage of wild type $\alpha_2\delta$-1, such that a mixture of cleaved and uncleaved $\alpha_2\delta$ protein appears in the whole cell lysate (WCL) (Kadurin et al. 2012, Kadurin et al. 2016). We performed co-immunoprecipitation of wild type $\alpha_2\delta$-1 with $Ca_V2.2$ from tsA-201 cell WCL and found that the percentage of cleaved $\alpha_2\delta$-1 in the co-immunoprecipitated fractions is ~ 4 fold higher than the percentage of cleaved $\alpha_2\delta$-1 in the input WCL (from 10.0 ± 0.6 % to 39.2 ± 1.6 % in WCL and co-immunoprecipitated fractions, respectively, n = 3) (Figure 4), suggesting stronger association of mature cleaved $\alpha_2\delta$-1 with the Ca_V pore-forming subunit.

Discussion

Ca_V2 channels are important for synaptic transmission and their targeting to the active zone is tightly regulated (Catterall & Few 2008, Simms & Zamponi 2014). $\alpha_2\delta$ subunits have been shown to control the trafficking of Ca_V2 to presynaptic terminals (Hoppa et al. 2012). $\alpha_2\delta$ subunits are post-translationally proteolysed, and this process is key for their regulatory action on Ca_V2 channels (Kadurin et al. 2016). Here we show that the post-translational

proteolytic maturation of $\alpha_2\delta$-1 is also essential for these proteins to fulfil their regulatory function on vesicular release in presynaptic terminals of hippocampal neurons in culture. Interestingly, we show that both synchronous and asynchronous releases are affected, both release mechanisms being highly dependent on Ca^{2+} influx through Ca_V2 channels.

Vesicular release is characterized by two key presynaptic parameters: the RRP and *Pv* (Ariel & Ryan 2012, Schneggenburger et al. 2002). A previous study has shown that over-expression of $\alpha_2\delta$ subunits and knock down of endogenous $\alpha_2\delta$ increased and decreased *Pv*, respectively (Hoppa et al. 2012). In good agreement with this, our data show that uncleaved $\alpha_2\delta$-1 (α_2(3C)δ-1) reduces *Pv*, and co-expression of the 3C-protease restores the control *Pv*. Interestingly, *Pv* is modulated by the number of Ca_V2 channels in each active zone (Ermolyuk et al. 2012) and we have previously shown that uncleaved $\alpha_2\delta$ subunits reduced the amplitude of calcium transients triggered by a single AP stimulation, by interfering with the trafficking of Ca_V2 channels (Kadurin et al. 2016). The active zone proteins Rab-3 Interacting Molecules (RIMs) and Munc-13, critical in the orchestration of synaptic vesicular release, have been shown to control the targeting of Ca_V2 channels within presynaptic terminals (de Jong et al. 2018, Sudhof 2012). These active zone proteins have also been shown to control the size of the RRP (Augustin et al. 1999, Calloway et al. 2015, Deng et al. 2011, Kaeser et al. 2011). The RRP is defined as a small fraction of vesicles in a presynaptic terminal that is available for immediate release with a brief stimulus train, and thus likely to equate to docked vesicles identified by electron microscopy (Ariel & Ryan 2012, Rizzoli & Betz 2005, Schneggenburger et al. 2002). Experimental methods used to estimate the size of the RRP have been recently reviewed and consist of two electrophysiological methods (post synaptic current recordings and presynaptic membrane capacitance measurements) and one optical method (Kaeser & Regehr 2017). Here, we used the optical technique that was developed by Ariel & Ryan (2010). This high-time resolution optical method measures exocytosis by detecting fluorescence from pHluorin tagged vGlut-1

(Voglmaier et al. 2006) associated with vesicle fusion. The high frequency stimulation protocol (20 APs at 100 Hz) induces a rapid rise in fluorescence followed by a plateau corresponding to a state during which all the vesicles in the RRP have fused with the membrane. The size of the RRP we describe here, which is determined by the amplitude of the fluorescence of the plateau (6-7 % of the total pool of vesicles) is in good agreement with previously described values of RRP in neonatal rodent hippocampal neuron synapses (Ariel & Ryan 2010, Fernandez-Alfonso & Ryan 2006, Rizzoli & Betz 2005). A previous study has shown that wild-type $\alpha_2\delta$ subunits have no effect on the size of the RRP (Hoppa et al. 2012). Consistent with this study, our data shows that uncleaved $\alpha_2\delta$-1 does not affect the size of the RRP indicating that, unlike RIMs & Munc13, $\alpha_2\delta$-1 does not have the same dual function on synaptic vesicular release.

There are two potential mechanisms to account for the reduction in *Pv* by α_2(3C)δ-1. It is likely that α_2(3C)δ-1 reduces the trafficking of endogenous Ca_V2 channels into active zones, as we showed for exogenously expressed $Ca_V2.2$ (Kadurin et al. 2016). However, α_2(3C)δ-1 can also traffic alone into presynaptic terminals (Kadurin et al. 2016), where it could then displace the endogenous $\alpha_2\delta$ interacting with channels in active zones, thus forming non-functional channels. The finding here that uncleaved $\alpha_2\delta$ interacts less than cleaved $\alpha_2\delta$ with $Ca_V2.2$ may indicate that the former mechanism is more likely.

Several reports have also described a role for $\alpha_2\delta$ subunits in synaptogenesis, independently from their role as a Ca_V auxiliary subunit (Dickman et al. 2008, Eroglu et al. 2009, Kurshan et al. 2009). $\alpha_2\delta$ subunits are extracellular proteins anchored to the plasma membrane via a GPI moiety (Davies et al. 2010) which makes them potentially good candidates to interact with extracellular ligands such as thrombospondins, low density lipoprotein receptor-related protein and α-neurexin (Eroglu et al. 2009, Kadurin et al. 2017, Tong et al. 2017). Although a direct interaction between $\alpha_2\delta$ and thrombospondin and its role in the mediation of

synaptogenesis remains controversial (Lana et al. 2016, Xu et al. 2010), altogether these reports suggest that $\alpha_2\delta$ subunits could play a role as an extracellular coordinator of synaptic function. Furthermore, the modulation of presynaptic Ca_V channels by proteolytic cleavage of $\alpha_2\delta$ subunits could serve as an additional regulatory mechanism for their complex synaptic functions at the post-translational level.

Ca_V2 channels and BK potassium channels are known to be part of multi-molecular complexes in neurons (Berkefeld et al. 2006, Muller et al. 2010). $\alpha_2\delta$-1 has very recently been shown to interact with BK channels, and this interaction was found to reduce the stability of $Ca_V2.2$ channels at the plasma membrane by preventing $\alpha_2\delta$-1 interacting with $Ca_V2.2$ channels (Zhang et al. 2018). Functionally, BK channels were shown to control neurotransmitter release by shortening the AP duration and reducing Ca^{2+} influx into presynaptic elements at neuro-muscular junctions (Protti & Uchitel 1997, Yazejian et al. 1997). Although their presence in presynaptic boutons has been disputed (Hoppa et al. 2014), BK channels are also expressed in axons from central neurons (Debanne et al. 2011, Johnston et al. 2010). Furthermore, $\alpha_2\delta$-1 has also recently been shown to interact with NMDA glutamate receptors (NMDARs) (Chen et al. 2018), albeit via a C-terminal domain of $\alpha_2\delta$-1 that is beyond the GPI-anchor attachment site and would therefore not be present in a mature GPI-anchored form (Davies et al. 2010, Kadurin et al. 2012, Wu et al. 2016). This interaction was found to promote the trafficking of the NMDARs to synaptic sites between peripheral dorsal root ganglion neurons and dorsal horn neurons in the spinal cord and is involved in the development of neuropathic pain (Chen et al. 2018). Therefore, it will be of great interest to determine whether fully mature $\alpha_2\delta$-1 is required for the interaction with BK potassium channels and with NMDARs.

Synchronous stimulated release is often followed by a delayed release occurring after the end of the stimulus, also called asynchronous release (Atluri & Regehr 1998, Goda &

Stevens 1994, Kaeser & Regehr 2014). Asynchronous release is thought to be activated by residual Ca^{2+} remaining in the presynaptic terminal after the stimulation (Atluri & Regehr 1998, Cummings et al. 1996). Although the source of Ca^{2+} responsible for the initiation of synchronous release is indisputably identified from many studies as voltage-gated calcium channels within the active zone (Catterall & Few 2008, Dolphin 2012, Nakamura et al. 2015, Zamponi et al. 2015), the source of Ca^{2+} involved in asynchronous release remains uncertain. To study asynchronous release in this work, we took advantage of the optical method developed previously (Ariel & Ryan 2010) to monitor the slow increase of fluorescence of pHluorin tagged to vGlut-1 after the end of the high frequency stimulation (20 AP at 100Hz). We show that asynchronous release is reduced in hippocampal presynaptic terminals when uncleaved $\alpha_2\delta$-1 (α_2(3C)δ-1) is expressed, and this inhibitory effect is abolished when 3C-protease is co-expressed. Together with our previous report showing that the proteolytic cleavage of $\alpha_2\delta$ is critical for the functional trafficking of $Ca_V2.2$ channels to the presynaptic terminals (Kadurin et al. 2016), our data demonstrate that asynchronous release is mediated by Ca^{2+} influx generated by Ca_V localized at the presynaptic terminals. Relevant to our data, a study has characterized an asynchronous Ca^{2+} current, recorded after the end of the stimulation pulse, conducted by both $Ca_V2.1$ and $Ca_V2.2$ channels and activated by the increase of intracellular Ca^{2+} generated by the activity of these channels (Few et al. 2012). This asynchronous current was also identified in mouse hippocampal neurons and this led the authors to suggest that the asynchronous current could contribute to asynchronous release (Few et al. 2012). Other Ca^{2+} sources for asynchronous release have been proposed (Kaeser & Regher 2014). Ca^{2+}-permeable P2X2 ATP receptors have been involved in asynchronous release in excitatory synapses between CA3 neurons and interneurons in the CA1 region in the hippocampus (Khakh 2009). At these synapses, P2X2 receptors would be activated by ATP released from vesicles in presynaptic terminals. Further pharmacological characterization would be needed to ascertain the involvement of

P2X2 receptors in the asynchronous release we are monitoring in our experimental model. Additionally, in the nucleus of the solitary tract, TRPV1 channels had been suggested to be a source of Ca^{2+} for asynchronous release at excitatory synapses from unmyelinated cranial visceral primary afferent neurons (Peters et al. 2010). However recent data from the same group have suggested instead that the Ca^{2+} source for asynchronous release would originate from spill-over of intracellular Ca^{2+} from Ca^{2+} nanodomains created by Ca_V2 channels (Fawley et al. 2016). This latter hypothesis would fit well with our data showing that mature $\alpha_2\delta$-1 is needed to traffic Ca_V to the presynaptic terminals to modulate asynchronous release.

Building on our previous report, we show here that the maturation of $\alpha_2\delta$ is crucial for Ca_V channels to fulfil their functional role on synaptic transmission. As $\alpha_2\delta$-1 expression is upregulated during chronic pain and increases presynaptic Ca_V2 trafficking (Bauer et al. 2009, Kadurin et al. 2016, Patel et al. 2013, Zamponi et al. 2015), $\alpha_2\delta$-1 represents a therapeutic target (Zamponi 2016), and an important question to address for future studies will be to identify endogenous protease(s) involved in the proteolytic maturation of $\alpha_2\delta$ proteins.

Materials & Methods

Neuronal culture and transfection

All experiments were performed in accordance with the Home Office Animals (Scientific procedures) Act 1986, UK, using a Schedule 1 method. Hippocampal neurons were obtained from male P0 Sprague Dawley rat pups as previously described (Hoppa et al. 2012). Approximately 75 × 10^3 cells in 200 μl of plating medium (MEM (Thermo Fisher Scientific) supplemented with B27 (Thermo Fisher Scientific, 2%), glucose (Sigma, 5 mg/ml), transferrin (Millipore, 100 μg/ml), insulin (Sigma, 24 μg/ml), fetal bovine serum (Thermo Fisher Scientific, 10%), GlutaMax (Thermo Fisher Scientific,1%)) were seeded onto sterile poly-L-ornithine-coated glass coverslips. After 24 h, the plating medium was replaced with feeding medium (MEM supplemented with B27 (2%), glucose (5 mg/ml), transferrin (100 μg/ml), insulin (24 μg/ml), Fetal bovine serum (5%), GlutaMax (1%) and cytosine arabinose (Sigma, 0.4 μM)) half of which was replaced every 7 days. At 7 days in vitro (DIV) and 2 h before transfection, half of the medium was removed, and kept as 'conditioned' medium, and fresh medium was added. The hippocampal cell cultures were then transfected with mCherry, vGlut-pHluorin and either empty vector or α_2(3C)δ−1 or α_2(3C)δ−1 + 3C-protease (all cloned in pCAGGs) using Lipofectamine 2000 (Thermo Fisher scientific). After 2 h, the transfection mixes were replaced with feeding medium consisting of 50% 'conditioned' and 50% fresh medium.

Co-Immunoprecipitation

The protocol was adapted from a procedure described previously (Gurnett et al. 1997). Briefly, a tsA-201 cell pellet derived from one confluent 75-cm^2 flask was resuspended in co-IP buffer (20 mM HEPES (pH 7.4), 300 mM NaCl, 1 % Digitonin and PI), sonicated for 8 s at 20 kHz and rotated for 1 h at 4 °C. The samples were then diluted with an equal volume of 20 mM HEPES (pH 7.4), 300 mM NaCl with PI (to 0.5 % final concentration of Digitonin),

mixed by pipetting and centrifuged at 20,000 x g for 20 min. The supernatants were collected and assayed for total protein (Bradford assay; Biorad). 1 mg of total protein was adjusted to 2 mg/ml with co-IP buffer and incubated overnight at 4 °C with anti-GFP polyclonal antibody (1:200; BD Biosciences). 30 µl A/G PLUS Agarose slurry (Santa Cruz) was added to each tube and further rotated for 2 h at 4 °C. The beads were then washed three times with co-IP buffer containing 0.2 % Digitonin and deglycosylated as previously described alongside with aliquots of the initial WCL prior to co-IP. Laemmli buffer with 100 mM DTT was added to 1 x final concentration and samples were analysed by SDS-PAGE and Western blotting with the indicated antibodies as described previously (Kadurin et al. 2016).

The human embryonic kidney tsA-201 cells were obtsined from the European Collection of Authenticated Cell Cultures (# 96121229) and tested to be mycoplasma-free.

Live cell imaging

Coverslips were mounted in a rapid-switching, laminar-flow perfusion and stimulation chamber (RC-21BRFS, Warner Instruments) on the stage of an epifluorescence microscope (Axiovert 200M, Zeiss). Live cell images were acquired with an Andor iXon+ (model DU-897U-CS0-BV) back-illuminated EMCCD camera using OptoMorph software (Cairn Research, UK). White and 470nm LEDs served as light sources (Cairn Research, UK). Fluorescence excitation and collection was done through a Zeiss 40x1.3 NA Fluar objective using 450/50nm excitation and 510/50nm emission and 480nm dichroic filters (for pHluorin) and a 572/35nm excitation and low-pass 590nm emission and 580nm dichroic filters (for mCherry). Action potentials were evoked by passing 1 ms current pulses via platinum electrodes. Cells were perfused (0.5ml min^{-1}) in a saline solution at 32°C containing (in mM) 119 NaCl, 2.5 KCl, 4 $CaCl_2$, 25 HEPES (buffered to pH 7.4), 30 glucose, 10µM 6-cyano-7-nitroquinoxaline-2,3-dione (CNQX) and 50µM D,L-2-amino-5-phosphonovaleric acid (AP5, Sigma). NH_4Cl application was done with this solution in which 50mM NH_4Cl was substituted for 50mM NaCl (buffered to pH 7.4). Images were acquired at 100 Hz over a 512 x 266 pixel

area in frame transfer mode (exposure time 7ms) and analyzed in ImageJ (http://rsb.info.nih.gov/ij) using a custom-written plugin (http://rsb.info.nih.gov/ij/plugins/time-series.html). Regions of interest (ROI, 2 μm diameter circles) were placed around synaptic boutons responding to an electrical stimulation of 100 AP at 10 Hz.

Analysis

Data are given as mean ± SEM or as box (25–75%) and whiskers (10–90%) plots with mean and median (open squares and solid lines). Statistical comparisons were performed using unpaired Student's t test or one-way ANOVA with Bonferroni post-hoc test, using OriginPro 2016.

Acknowledgements

This work was supported by a Wellcome Trust Investigator award to ACD (098360/Z/12/Z)

We thank Dr. Matthew Gold for HRV-3C protease cDNA and Prof Tim Ryan (Weill Cornell Medical College) for providing vGlut-pHluorin.

Competing financial interests

The authors declare no competing financial interests

Supplementary File 1 Statistical information for Figures 1 – 3.

References

1 - Ariel P, Ryan TA. 2010. Optical mapping of release properties in synapses. *Front Neural Circuits* 4: 18. doi: 10.3389/fncir.2010.00018.

2 - Ariel P, Hoppa MB, Ryan TA. 2012. Intrinsic variability in Pv, RRP size, Ca(2+) channel repertoire, and presynaptic potentiation in individual synaptic boutons. *Front Synaptic Neurosci* 4: 9. doi: 10.3389/fnsyn.2012.00009.

3 - Ariel P, Ryan TA. 2012. New insights into molecular players involved in neurotransmitter release. *Physiology (Bethesda)* 27: 15-24.

4 - Atluri PP, Regehr WG. 1998. Delayed release of neurotransmitter from cerebellar granule cells. *J Neurosci* 18: 8214-27.

5 - Augustin I, Rosenmund C, Sudhof TC, Brose N. 1999. Munc13-1 is essential for fusion competence of glutamatergic synaptic vesicles. *Nature* 400: 457-61.

6 - Bauer CS, Nieto-Rostro M, Rahman W, Tran-Van-Minh A, Ferron L, et al. 2009. The increased trafficking of the calcium channel subunit alpha2delta-1 to presynaptic terminals in neuropathic pain is inhibited by the alpha2delta ligand pregabalin. *J Neurosci* 29: 4076-88.

7 - Berkefeld H, Sailer CA, Bildl W, Rohde V, Thumfart JO, et al. 2006. BKCa-Cav channel complexes mediate rapid and localized Ca2+-activated K+ signaling. *Science* 314: 615-20.

8 - Bourdin B, Briot J, Tetreault MP, Sauve R, Parent L. 2017. Negatively charged residues in the first extracellular loop of the L-type CaV1.2 channel anchor the interaction with the CaValpha2delta1 auxiliary subunit. *J Biol Chem* 292: 17236-49.

9 - Calloway N, Gouzer G, Xue M, Ryan TA. 2015. The active-zone protein Munc13 controls the use-dependence of presynaptic voltage-gated calcium channels. *Elife* 4

10 - Canti C, Nieto-Rostro M, Foucault I, Heblich F, Wratten J, et al. 2005. The metal-ion-dependent adhesion site in the Von Willebrand factor-A domain of alpha2delta subunits is key to trafficking voltage-gated Ca2+ channels. *Proc Natl Acad Sci U S A* 102: 11230-5.

11 - Catterall WA, Few AP. 2008. Calcium channel regulation and presynaptic plasticity. *Neuron* 59: 882-901.

12 - Chen J, Li L, Chen SR, Chen H, Xie JD, et al. 2018. The alpha2delta-1-NMDA Receptor Complex Is Critically Involved in Neuropathic Pain Development and Gabapentin Therapeutic Actions. *Cell Rep* 22: 2307-21.

13 - Cummings DD, Wilcox KS, Dichter MA. 1996. Calcium-dependent paired-pulse facilitation of miniature EPSC frequency accompanies depression of EPSCs at hippocampal synapses in culture. *J Neurosci* 16: 5312-23.

14 - Davies A, Kadurin I, Alvarez-Laviada A, Douglas L, Nieto-Rostro M, et al. 2010. The alpha2delta subunits of voltage-gated calcium channels form GPI-anchored proteins, a posttranslational modification essential for function. *Proc Natl Acad Sci U S A* 107: 1654-9.

15 - de Jong APH, Roggero CM, Ho MR, Wong MY, Brautigam CA, et al. 2018. RIM C2B Domains Target Presynaptic Active Zone Functions to PIP2-Containing Membranes. *Neuron*

16 - Debanne D, Campanac E, Bialowas A, Carlier E, Alcaraz G. 2011. Axon physiology. *Physiol Rev* 91: 555-602.

17 - Deng L, Kaeser PS, Xu W, Sudhof TC. 2011. RIM proteins activate vesicle priming by reversing autoinhibitory homodimerization of Munc13. *Neuron* 69: 317-31.

18 - Dickman DK, Kurshan PT, Schwarz TL. 2008. Mutations in a Drosophila alpha2delta voltage-gated calcium channel subunit reveal a crucial synaptic function. *J Neurosci* 28: 31-8.

19 - Dolphin AC. 2012. Calcium channel auxiliary alpha2delta and beta subunits: trafficking and one step beyond. *Nat Rev Neurosci* 13: 542-55.

20 - Ermolyuk YS, Alder FG, Henneberger C, Rusakov DA, Kullmann DM, Volynski KE. 2012. Independent regulation of basal neurotransmitter release efficacy by variable Ca(2)+ influx and bouton size at small central synapses. *PLoS Biol* 10: e1001396.
21 - Eroglu C, Allen NJ, Susman MW, O'Rourke NA, Park CY, et al. 2009. Gabapentin receptor alpha2delta-1 is a neuronal thrombospondin receptor responsible for excitatory CNS synaptogenesis. *Cell* 139: 380-92.
22 - Fawley JA, Hofmann ME, Andresen MC. 2016. Distinct Calcium Sources Support Multiple Modes of Synaptic Release from Cranial Sensory Afferents. *J Neurosci* 36: 8957-66.
23 - Fernandez-Alfonso T, Ryan TA. 2006. The efficiency of the synaptic vesicle cycle at central nervous system synapses. *Trends Cell Biol* 16: 413-20.
24 - Few AP, Nanou E, Watari H, Sullivan JM, Scheuer T, Catterall WA. 2012. Asynchronous Ca2+ current conducted by voltage-gated Ca2+ (CaV)-2.1 and CaV2.2 channels and its implications for asynchronous neurotransmitter release. *Proc Natl Acad Sci U S A* 109: E452-60.
25 - Flockerzi V, Oeken HJ, Hofmann F, Pelzer D, Cavalie A, Trautwein W. 1986. Purified dihydropyridine-binding site from skeletal muscle t-tubules is a functional calcium channel. *Nature* 323: 66-8.
26 - Goda Y, Stevens CF. 1994. Two components of transmitter release at a central synapse. *Proc Natl Acad Sci U S A* 91: 12942-6.
27 - Gurnett CA, Felix R, Campbell KP. 1997. Extracellular interaction of the voltage-dependent Ca2+ channel alpha2delta and alpha1 subunits. *J Biol Chem* 272: 18508-12.
28 - Hendrich J, Van Minh AT, Heblich F, Nieto-Rostro M, Watschinger K, et al. 2008. Pharmacological disruption of calcium channel trafficking by the alpha2delta ligand gabapentin. *Proc Natl Acad Sci U S A* 105: 3628-33.
29 - Hoppa MB, Lana B, Margas W, Dolphin AC, Ryan TA. 2012. alpha2delta expression sets presynaptic calcium channel abundance and release probability. *Nature* 486: 122-5.
30 - Hoppa MB, Gouzer G, Armbruster M, Ryan TA. 2014. Control and plasticity of the presynaptic action potential waveform at small CNS nerve terminals. *Neuron* 84: 778-89.
31 - Johnston J, Forsythe ID, Kopp-Scheinpflug C. 2010. Going native: voltage-gated potassium channels controlling neuronal excitability. *J Physiol* 588: 3187-200.
32 - Kadurin I, Alvarez-Laviada A, Ng SF, Walker-Gray R, D'Arco M, et al. 2012. Calcium currents are enhanced by alpha2delta-1 lacking its membrane anchor. *J Biol Chem* 287: 33554-66.
33 - Kadurin I, Ferron L, Rothwell SW, Meyer JO, Douglas LR, et al. 2016. Proteolytic maturation of alpha2delta represents a checkpoint for activation and neuronal trafficking of latent calcium channels. *Elife* 5
34 - Kadurin I, Rothwell SW, Lana B, Nieto-Rostro M, Dolphin AC. 2017. LRP1 influences trafficking of N-type calcium channels via interaction with the auxiliary alpha2delta-1 subunit. *Sci Rep* 7: 43802.
35 - Kaeser PS, Deng L, Wang Y, Dulubova I, Liu X, et al. 2011. RIM proteins tether Ca2+ channels to presynaptic active zones via a direct PDZ-domain interaction. *Cell* 144: 282-95.
36 - Kaeser PS, Regehr WG. 2014. Molecular mechanisms for synchronous, asynchronous, and spontaneous neurotransmitter release. *Annu Rev Physiol* 76: 333-63.
37 - Kaeser PS, Regehr WG. 2017. The readily releasable pool of synaptic vesicles. *Curr Opin Neurobiol* 43: 63-70.
38 - Khakh BS. 2009. ATP-gated P2X receptors on excitatory nerve terminals onto interneurons initiate a form of asynchronous glutamate release. *Neuropharmacology* 56: 216-22.

450 39 - Kurshan PT, Oztan A, Schwarz TL. 2009. Presynaptic alpha2delta-3 is required for
451 synaptic morphogenesis independent of its Ca2+-channel functions. *Nat Neurosci* 12:
452 1415-23.
453 40 - Lana B, Page KM, Kadurin I, Ho S, Nieto-Rostro M, Dolphin AC. 2016.
454 Thrombospondin-4 reduces binding affinity of [(3)H]-gabapentin to calcium-channel
455 alpha2delta-1-subunit but does not interact with alpha2delta-1 on the cell-surface when
456 co-expressed. *Sci Rep* 6: 24531.
457 41 - Liu H, De Waard M, Scott VE, Gurnett CA, Lennon VA, Campbell KP. 1996.
458 Identification of three subunits of the high affinity omega-conotoxin MVIIC-sensitive
459 Ca2+ channel. *J Biol Chem* 271: 13804-10.
460 42 - Muller CS, Haupt A, Bildl W, Schindler J, Knaus HG, et al. 2010. Quantitative
461 proteomics of the Cav2 channel nano-environments in the mammalian brain. *Proc Natl*
462 *Acad Sci U S A* 107: 14950-7.
463 43 - Nakamura Y, Harada H, Kamasawa N, Matsui K, Rothman JS, et al. 2015. Nanoscale
464 distribution of presynaptic Ca(2+) channels and its impact on vesicular release during
465 development. *Neuron* 85: 145-58.
466 44 - Patel R, Bauer CS, Nieto-Rostro M, Margas W, Ferron L, et al. 2013. alpha2delta-1
467 gene deletion affects somatosensory neuron function and delays mechanical
468 hypersensitivity in response to peripheral nerve damage. *J Neurosci* 33: 16412-26.
469 45 - Peters JH, McDougall SJ, Fawley JA, Smith SM, Andresen MC. 2010. Primary afferent
470 activation of thermosensitive TRPV1 triggers asynchronous glutamate release at central
471 neurons. *Neuron* 65: 657-69.
472 46 - Protti DA, Uchitel OD. 1997. P/Q-type calcium channels activate neighboring calcium-
473 dependent potassium channels in mouse motor nerve terminals. *Pflugers Arch* 434:
474 406-12.
475 47 - Rizzoli SO, Betz WJ. 2005. Synaptic vesicle pools. *Nat Rev Neurosci* 6: 57-69.
476 48 - Saheki Y, Bargmann CI. 2009. Presynaptic CaV2 calcium channel traffic requires CALF-
477 1 and the alpha(2)delta subunit UNC-36. *Nat Neurosci* 12: 1257-65.
478 49 - Schneggenburger R, Sakaba T, Neher E. 2002. Vesicle pools and short-term synaptic
479 depression: lessons from a large synapse. *Trends Neurosci* 25: 206-12.
480 50 - Simms BA, Zamponi GW. 2014. Neuronal voltage-gated calcium channels: structure,
481 function, and dysfunction. *Neuron* 82: 24-45.
482 51 - Sudhof TC. 2012. The presynaptic active zone. *Neuron* 75: 11-25.
483 52 - Takahashi M, Catterall WA. 1987. Identification of an alpha subunit of dihydropyridine-
484 sensitive brain calcium channels. *Science* 236: 88-91.
485 53 - Tong XJ, Lopez-Soto EJ, Li L, Liu H, Nedelcu D, et al. 2017. Retrograde Synaptic
486 Inhibition Is Mediated by alpha-Neurexin Binding to the alpha2delta Subunits of N-Type
487 Calcium Channels. *Neuron* 95: 326-40 e5.
488 54 - Voglmaier SM, Kam K, Yang H, Fortin DL, Hua Z, et al. 2006. Distinct endocytic
489 pathways control the rate and extent of synaptic vesicle protein recycling. *Neuron* 51:
490 71-84.
491 55 - Witcher DR, De Waard M, Sakamoto J, Franzini-Armstrong C, Pragnell M, et al. 1993.
492 Subunit identification and reconstitution of the N-type Ca2+ channel complex purified
493 from brain. *Science* 261: 486-9.
494 56 - Wu J, Yan Z, Li Z, Qian X, Lu S, et al. 2016. Structure of the voltage-gated calcium
495 channel Ca(v)1.1 at 3.6 A resolution. *Nature* 537: 191-96.
496 57 - Xu J, Xiao N, Xia J. 2010. Thrombospondin 1 accelerates synaptogenesis in
497 hippocampal neurons through neuroligin 1. *Nat Neurosci* 13: 22-4.
498 58 - Yazejian B, DiGregorio DA, Vergara JL, Poage RE, Meriney SD, Grinnell AD. 1997.
499 Direct measurements of presynaptic calcium and calcium-activated potassium currents
500 regulating neurotransmitter release at cultured Xenopus nerve-muscle synapses. *J*
501 *Neurosci* 17: 2990-3001.

59 - Zamponi GW, Striessnig J, Koschak A, Dolphin AC. 2015. The Physiology, Pathology, and Pharmacology of Voltage-Gated Calcium Channels and Their Future Therapeutic Potential. *Pharmacol Rev* 67: 821-70.
60 - Zamponi GW. 2016. Targeting voltage-gated calcium channels in neurological and psychiatric diseases. *Nat Rev Drug Discov* 15: 19-34.
61 - Zhang FX, Gadotti VM, Souza IA, Chen L, Zamponi GW. 2018. BK Potassium Channels Suppress Cavalpha2delta Subunit Function to Reduce Inflammatory and Neuropathic Pain. *Cell Rep* 22: 1956-64.

Figure legends

Figure 1. Effect of proteolytic cleavage of a_2(3C)d-1 on vesicular release in presynaptic terminals of hippocampal neurons.

a) Fluorescence changes in presynaptic terminals of hippocampal neurons expressing vGlut-pHluorin (vG-pHluorin) in response to electrical stimulation. Left panel, mCherry-positive boutons. Three right panels, vG-pHluorin fluorescence: at rest (left), after 100 AP at 10 Hz (middle) and after a brief application of NH_4Cl (right). Scale bar 5 µm. The pseudocolour scale is shown on the first panel. b) Representative vG-pHluorin responses to a single AP (10-12 trial average, 25 to 50 boutons) from presynaptic terminals of neurons co-transfected with empty vector (black trace), a_2(3C)d-1 (red trace) or a_2(3C)d-1 + 3C-protease (blue trace). Arrow indicates stimulation with one AP. c) vG-pHluorin fluorescence changes (expressed as % of NH_4Cl response) in response to 1 AP from boutons co-transfected with empty vector (black), a_2(3C)d-1 (red) or a_2(3C)d-1 + 3C-protease (blue) (n = 28, 41 and 16 independent experiments, respectively). Box and whiskers plots; $^{*}P = 0.044$ and $^{\#}P = 0.014$, one way ANOVA and Bonferroni post-hoc test.

Figure 2. The proteolytic cleavage of a_2(3C)d-1 does not affect the readily releasable pool (RRP) in presynaptic terminals of hippocampal neurons.

a-c) vG-pHluorin responses (mean ± SEM) to 20 AP at 100 Hz (5-6 trial average, 25 to 50 boutons) from presynaptic terminals of neurons co-transfected with empty vector (a), a_2(3C)d-1 (b) or a_2(3C)d-1+ 3C-protease (c). Horizontal red lines identify RRPs. d) Average RRP (expressed as % of NH_4Cl response) from boutons co-transfected with empty vector (black), a_2(3C)d-1 (red) or a_2(3C)d-1 + 3C-protease (blue) (n = 22, 16 and 19 independent experiments, respectively, P = 0.78). Box and whiskers plots; one way ANOVA and Bonferroni post-hoc test.

Figure 3. Effect of the proteolytic cleavage of a_2(3C)d-1 on delayed vesicular release in presynaptic terminals of hippocampal neurons. a) Average vG-pHluorin responses (mean ± SEM) to 20 APs at 100 Hz (5-6 trial average, 25 to 50 boutons) from presynaptic terminals of neurons co-transfected with empty vector (black), a_2(3C)d-1 (red) or a_2(3C)d-1 + 3C-protease (blue). The black bar indicates the stimulation period (20 AP at 100 Hz). b) Average delayed vesicular release (expressed as % of NH_4Cl response) measured 1 s after the beginning of the stimulation from boutons co-transfected with empty vector (black),

543 a_2(3C)d-1 (red) or a_2(3C)d-1 + 3C-protease (blue) (n = 22, 31 and 15 independent
544 experiments, respectively). Box and whiskers plots with superimposed individual
545 experiments; ***P < 0.001 and # P = 0.021, one way ANOVA and Bonferroni post-hoc test.

546 **Figure 4. Quantified co-immunoprecipitation of $Ca_V2.2$ with cleaved and uncleaved**
547 **fractions of wild-type a_2d-1 from WCL of tsA-201 cells.** a) Left panels show WCL input
548 from tsA-201 cells transfected with GFP-$Ca_V2.2$ (lanes 1 and 2) or GFP (lane 3), plus β1b
549 and HA-tagged a_2d-1: upper panel, HA-a_2d-1 input; lower panel, $Ca_V2.2$-GFP input. Right
550 panels show immunoprecipitation (IP) of GFP-$Ca_V2.2$ with anti-GFP Ab; immunoblots
551 with $Ca_V2.2$ II-III loop Ab (lower panels, lanes 4 and 5) produced co-immunoprecipitation
552 (co-IP) of HA-a_2d-1 (corresponding upper panels lanes 4 and 5), revealed by anti-HA mAb.
553 All samples deglycosylated. b) Proteolytic cleavage of a_2d-1 expressed as percentage of
554 cleaved a_2-1 moiety to total a_2d-1 calculated for input WCL fractions (squares) and for
555 fractions co-immunoprecipitated with GFP- $Ca_V2.2$ (triangles). The cleaved a_2-1 moiety in
556 the co-IP fractions is increased by 29.2 ± 1.7 % compared with the WCL fractions (average
557 of 3 independent experiments). *** P = 0.0032, paired t-test.

558

559

560

561

562

563

Figure 1

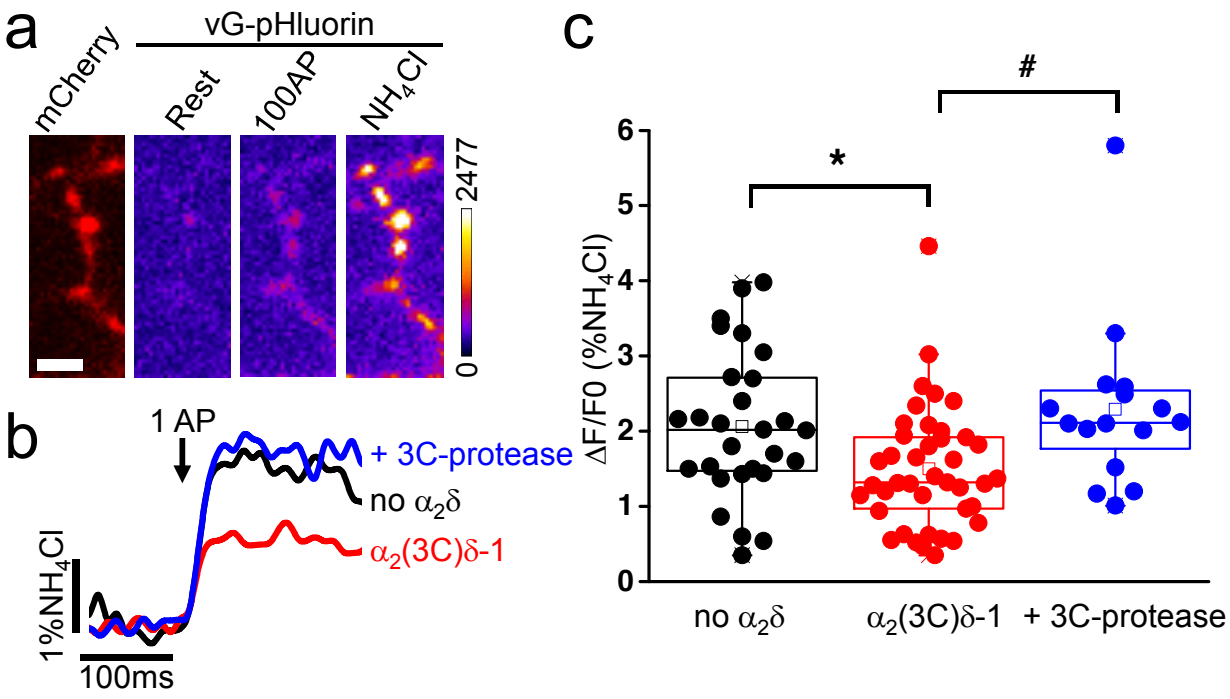

Effect of proteolytic cleavage of α_2(3C)δ-1 on vesicular release in presynaptic terminals of hippocampal neurons.

a) Fluorescence changes in presynaptic terminals of hippocampal neurons expressing vGlut-pHluorin (vG-pHluorin) in response to electrical stimulation. Left panel, mCherry-positive boutons. Three right panels, vG-pHluorin fluorescence: at rest (left), after 100 AP at 10 Hz (middle) and after a brief application of NH_4Cl (right). Scale bar 5 μm. The pseudocolour scale is shown on the first panel.

b) Representative vG-pHluorin responses to a single AP (10-12 trial average, 25 to 50 boutons) from presynaptic terminals of neurons co-transfected with empty vector (black trace), α_2(3C)δ-1 (red trace) or α_2(3C)δ-1 + 3C-protease (blue trace). Arrow indicates stimulation with one AP.

c) vG-pHluorin fluorescence changes (expressed as % of NH_4Cl response) in response to 1 AP from boutons co-transfected with empty vector (black), α_2(3C)δ-1 (red) or α_2(3C)δ-1 + 3C-protease (blue) (n = 28, 41 and 16 independent experiments, respectively). Box and whiskers plots; $^{*}P$ = 0.044 and $^{\#}P$ = 0.014, one way ANOVA and Bonferroni post-hoc test.

Figure 2

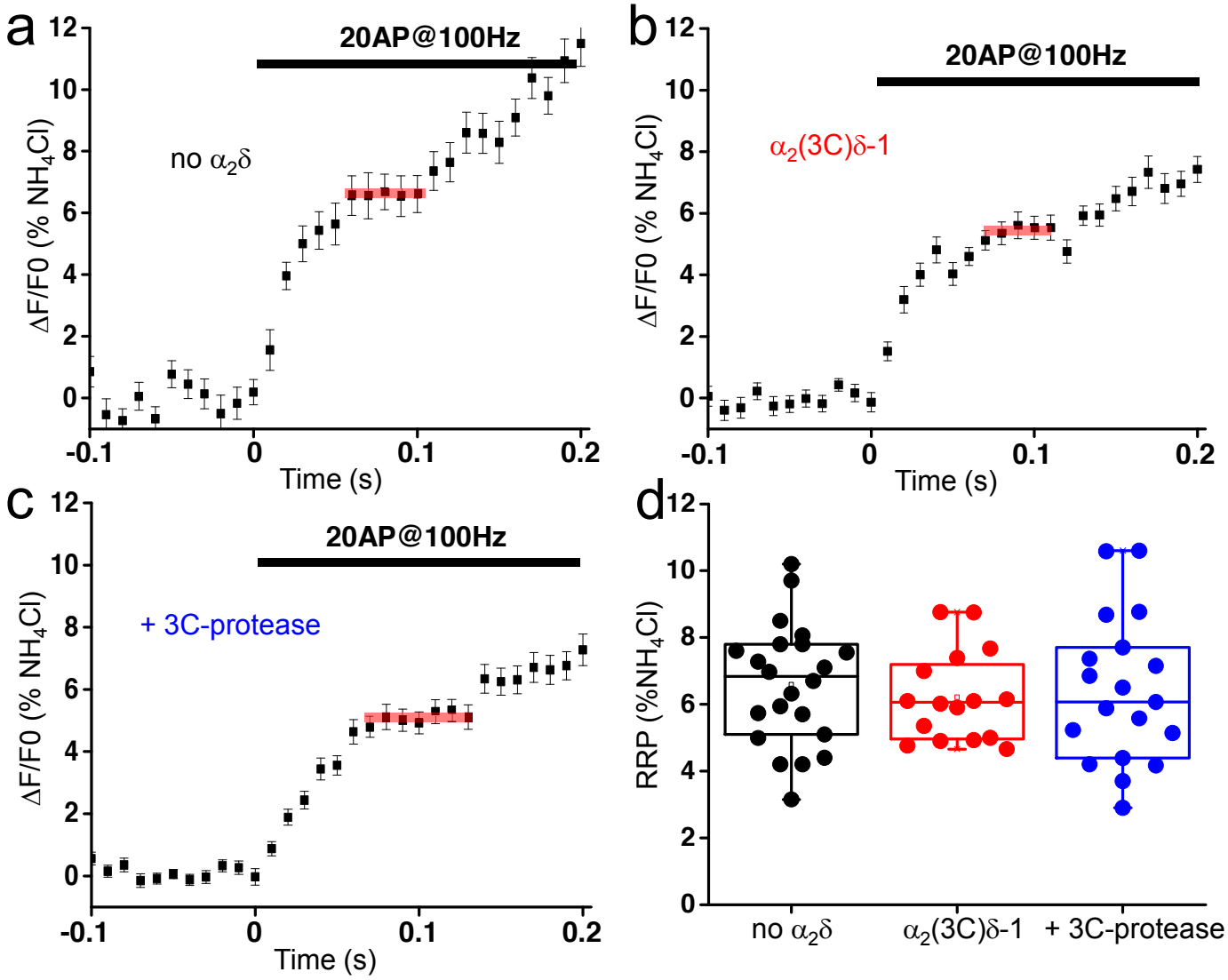

The proteolytic cleavage of α_2(3C)δ-1 does not affect the readily releasable pool (RRP) in presynaptic terminals of hippocampal neurons.

a-c) vG-pHluorin responses (mean ± SEM) to 20 AP at 100 Hz (5-6 trial average, 25 to 50 boutons) from presynaptic terminals of neurons co-transfected with empty vector (a), α_2(3C)δ-1 (b) or α_2(3C)δ-1+ 3C-protease (c). Horizontal red lines identify RRPs.

d) Average RRP (expressed as % of NH_4Cl response) from boutons co-transfected with empty vector (black), α_2(3C)δ-1 (red) or α_2(3C)δ-1 + 3C-protease (blue) (n = 22, 16 and 19 independent experiments, respectively, *P* = 0.78). Box and whiskers plots; one way ANOVA and Bonferroni post-hoc test.

Figure 3

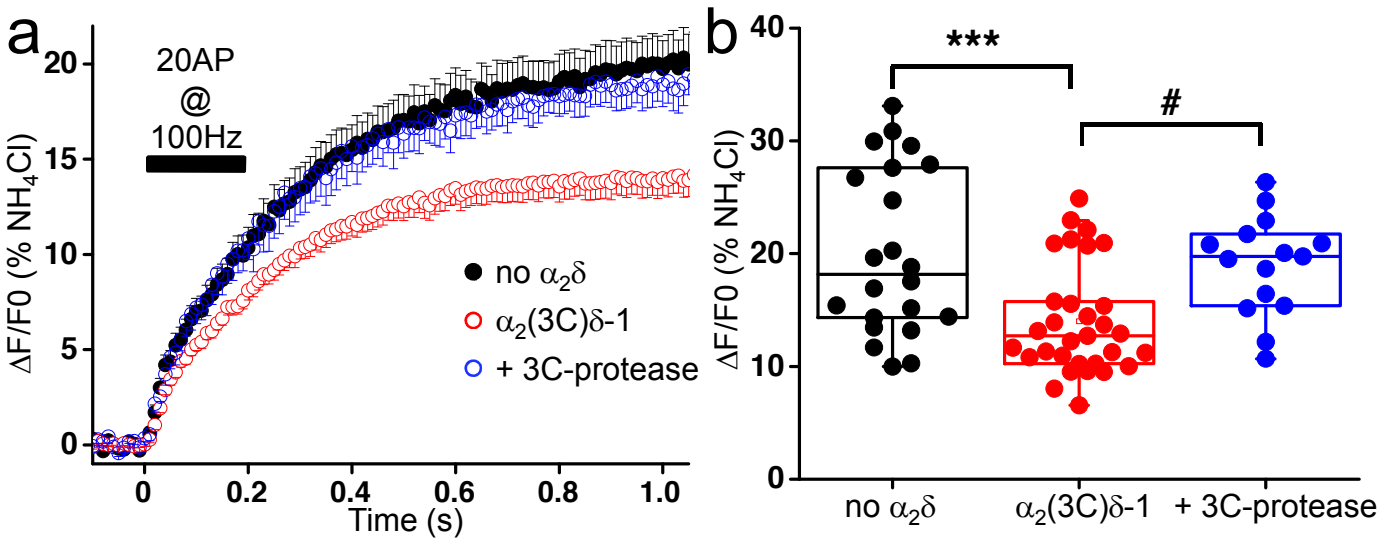

Effect of the proteolytic cleavage of α_2(3C)δ-1 on delayed vesicular release in presynaptic terminals of hippocampal neurons.

a) Average vG-pHluorin responses (mean ± SEM) to 20 APs at 100 Hz (5-6 trial average, 25 to 50 boutons) from presynaptic terminals of neurons co-transfected with empty vector (black), α_2(3C)δ-1 (red) or α_2(3C)δ-1 + 3C-protease (blue). The black bar indicates the stimulation period (20 AP at 100 Hz).

b) Average delayed vesicular release (expressed as % of NH_4Cl response) measured 1 s after the beginning of the stimulation from boutons co-transfected with empty vector (black), α_2(3C)δ-1 (red) or α_2(3C)δ-1 + 3C-protease (blue) (n = 22, 31 and 15 independent experiments, respectively). Box and whiskers plots with superimposed individual experiments; ***$P < 0.001$ and $^{\#}$ $P = 0.021$, one way ANOVA and Bonferroni post-hoc test.

Figure 4

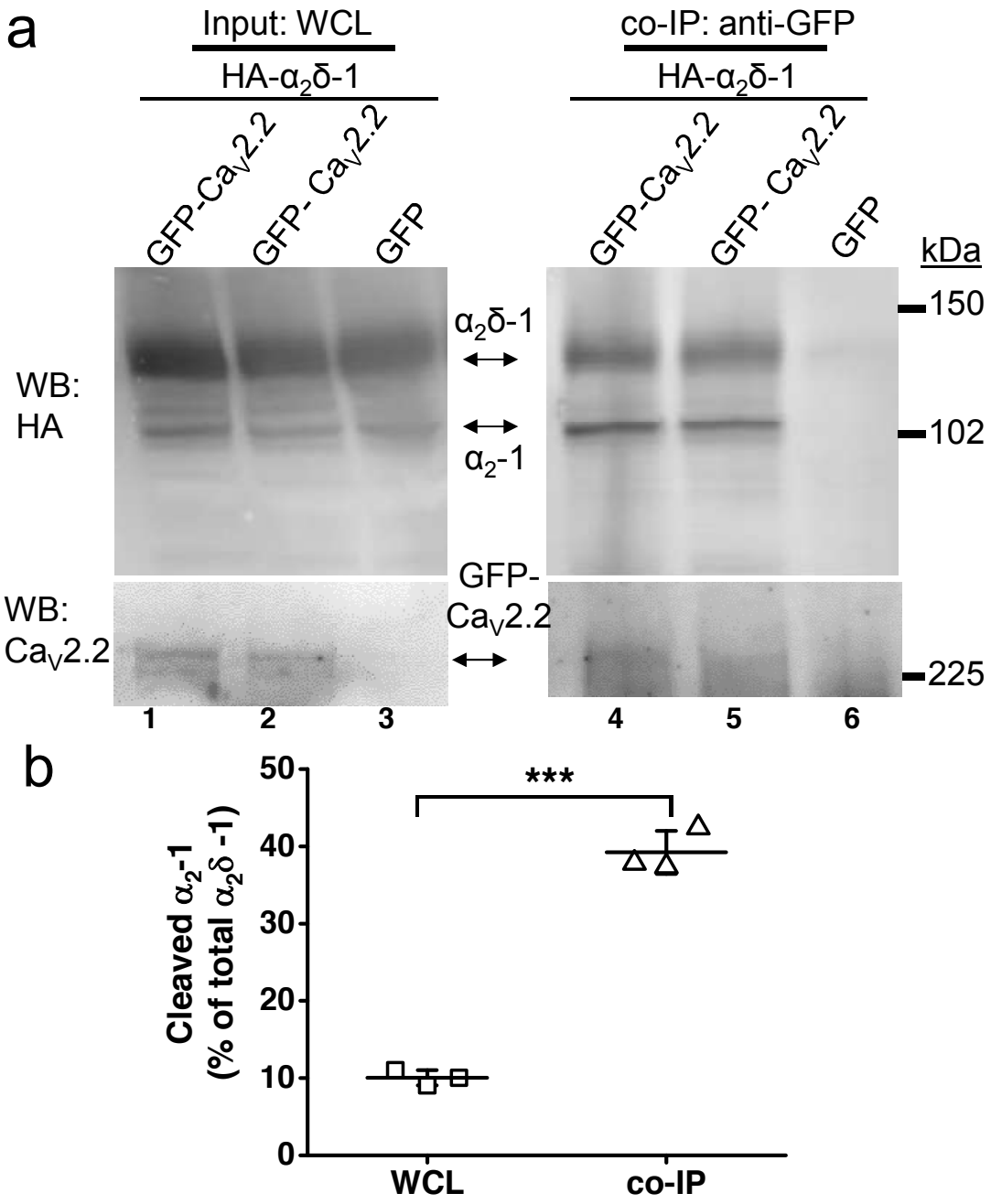

Quantified co-immunoprecipitation of $Ca_V2.2$ with cleaved and uncleaved fractions of wild-type $\alpha_2\delta$-1 from WCL of tsA-201 cells.

a) Left panels show WCL input from tsA-201 cells transfected with GFP-$Ca_V2.2$ (lanes 1 and 2) or GFP (lane 3), plus β1b and HA-tagged $\alpha_2\delta$-1: upper panel, HA-$\alpha_2\delta$-1 input; lower panel, $Ca_V2.2$-GFP input. Right panels show immunoprecipitation (IP) of GFP-$Ca_V2.2$ with anti-GFP Ab; immunoblots with $Ca_V2.2$ II-III loop Ab (lower panels, lanes 4 and 5) produced co-immunoprecipitation (co-IP) of HA-$\alpha_2\delta$-1 (corresponding upper panels lanes 4 and 5), revealed by anti-HA mAb. All samples deglycosylated.

b) Proteolytic cleavage of $\alpha_2\delta$-1 expressed as percentage of cleaved α_2-1 moiety to total $\alpha_2\delta$-1 calculated for input WCL fractions (squares) and for fractions co-immunoprecipitated with GFP- $Ca_V2.2$ (triangles). The cleaved α_2-1 moiety in the co-IP fractions is increased by 29.2 ± 1.7 % compared with the WCL fractions (average of 3 independent experiments). *** P = 0.0032, paired t-test.